regeneration or repair of various impaired organs. Mesenchymal tissue from bone marrow, umbilical cord, and adipose tissue are relatively enriched with pluripotent stem cells.[12] Since the pathophysiological features of liver cirrhosis are a consequence of chronic hepatic inflammation, MSCs are especially suited to enhance regeneration and/or repair of damaged cirrhotic liver.

We have established a clinically relevant NASH cirrhotic murine model by feeding animals an atherogenic high-fat (Ath+HF) diet.[13] In this study we examined whether adipose-tissue-derived stem cells (ADSCs) can regenerate and/or repair the cirrhotic liver. We observed that injected ADSCs resided in the liver and expressed albumin, leading to restored albumin expression in hepatic parenchymal cells. ADSCs also ameliorated advanced fibrosis. Moreover, ADSCs suppressed the underlying persistent inflammation contributed by granulocytes, phagocytic cells, and T cells. These results suggest that treatment of patients with cirrhosis with ADSCs is a potentially novel approach for regenerating and/or repairing damaged cirrhotic liver tissue to restore hepatic function.

Materials and Methods

Culture of ADSCs. ADSCs were prepared as described.[14] Briefly, adipose tissue was obtained from the inguinal subcutaneous region of 10-week-old GFP-Tg male mice (a gift from Professor Okabe, Osaka University, Japan). The stem cell fraction was isolated from adipose tissue using type-I collagenase (Wako Pure Chemical Industries, Osaka, Japan) and cultured in Dulbecco's modified Eagle's medium: nutrient mixture F-12 supplemented with 10% heat-inactivated bovine serum albumin and 1% antibiotic-antimycotic solution. Cell culture reagents were purchased from Life Technologies (Carlsbad, CA).

NASH Murine Model. Female 8-week-old C57Bl/6J mice were purchased from Charles River Laboratories Japan (Yokohama, Japan). Mice were fed an Ath+HF diet composed of cocoa butter, cholesterol, cholate, and corticotropin-releasing factor-1 (Oriental Yeast Co., Tokyo, Japan) to induce steatohepatitis as reported previously.[13] Our Institutional Review Board approved the care and use of laboratory animals in all experiments.

ADSC Treatment of NASH Mice. ADSCs were harvested after six to eight passages in culture by treatment with trypsin/EDTA (Life Technologies) and passed through a 100-μm Cell Strainer mesh (BD Biosciences, San Jose, CA). Laparotomy was performed to inject 1×10^5 ADSCs or phosphate-buffered saline (PBS) into the splenic subcapsule. After ADSC treatment, the mice were anesthetized with pentobarbital (40 mg/kg; Kyoritsu Seiyaku, Tokyo, Japan), after which the liver was perfused with PBS and dissected. A portion of liver tissue was homogenized and incubated with type I collagenase (Wako Pure Chemical Industries), and hepatic parenchymal cells and inflammatory cells were separated with Percoll (GE Healthcare UK, Buckinghamshire, UK). $CD4^+$ T cells were isolated from hepatic inflammatory cells using a magnetic sorting system, the $CD4^+$ T cell Isolation Kit II (Miltenyi Biotec, Gladbach, Germany).

Histology and Immunohistochemical Staining. Liver tissue was preserved with formalin for paraffin embedding or embedded in OCT compound and frozen for sectioning (Sakura Finetek Japan, Tokyo, Japan). The frozen liver sections were fixed in acetone and endogenous peroxidase activity blocked with 3% hydrogen peroxide solution. After washing in PBS, the sections were incubated with a rabbit anti-CD11b antibody (BD Pharmingen, San Diego, CA) and a rabbit anti-Gr-1 antibody (eBioscience, San Diego, CA) overnight at 4°C. The slides were then washed and incubated with Histofine mouse MAXPO (Nichirei Bioscience, Tokyo, Japan) for 1 hour at room temperature. The immune complex was visualized by incubating with diaminobenzidine for 5 minutes. The paraffin-embedded sections were stained with a rabbit-anti-GFP antibody (Millipore, Billerica, MA), a rabbit anti-α-smooth muscle actin (α-SMA) antibody (Abcam, Cambridge, UK), and a rabbit anticollagen IV antibody (Abcam). Secondary antibody development was performed with diaminobenzidine as described above. In some experiments, the sliced

Address reprint requests to: Shuichi Kaneko, 13-1 Takara-machi, Kanazawa, Ishikawa 920-8641, Japan. E-mail: skaneko@m-kanazawa.jp; fax: +81-76-234-4250.

View this article online at wileyonlinelibrary.com.
DOI 10.1002/hep.26470
Potential conflict of interest: Nothing to report.
Additional Supporting Information may be found in the online version of this article.

sections were double-stained with a combination of a goat antimouse serum albumin antibody (Abcam) and a rabbit anti-GFP antibody followed by the secondary antibody and development as described above. To quantify fibrosis, paraffin-embedded sections were stained with Azan and viewed microscopically, after which the stained area was calculated using an image-analysis system (BIOREVO BZ-9000 and BZ-H1C, Keyence Japan, Osaka, Japan).

Flow Cytometry. Isolated hepatic inflammatory cells were incubated in PBS supplemented with 2% bovine serum albumin (Sigma-Aldrich, St. Louis, MO) for 10 minutes at 4°C. The cells were incubated with fluorescein isothiocyanate (FITC)-conjugated anti-CD4 (eBioscience) and phycoerythrin (PE)-conjugated anti-CD8 antibodies (eBioscience) for 30 minutes at 4°C before examination using a FACSCalibur cytometer (BD Biosciences). Similarly, ADSCs were incubated with PE-conjugated CD90 (Beckman Coulter, Fullerton, CA), or PE-conjugated CD105 (Miltenyi Biotec). The data were analyzed using the FlowJo software (Tree Star, Ashland, OR).

DNA Microarray Analysis. Isolated RNAs were amplified and labeled with Cy3 using a QuickAmp Labeling Kit (Agilent Technologies, Santa Clara, CA) in accordance with the manufacturer's protocol. cRNA (825 ng) was hybridized onto a Whole Mouse Genome 4 × 44K Array (Agilent Technologies). The hybridized microarray slide was scanned using a DNA microarray scanner (model G2505B; Agilent Technologies).

Gene expression analysis was carried out using GeneSpring analysis software (Agilent Technologies). Each measurement was divided by the 75th percentile of all measurements in that sample to normalize per chip. Hierarchical clustering and principal component analysis of gene expression was performed. Welch's *t* test with Benjamini and Hochberg's false-discovery rate were used to identify differentially expressed genes in the groups of interest. Analysis of biological processes was performed using the MetaCore software suite (GeneGo, San Diego, CA). BRB array tools (http://linus.nci.nih.gov/BRB-ArrayTools.html) were also used for unsupervised clustering or one-way clustering analysis. Microarray data were deposited in the NBCI Gene Expression Omnibus (GSE ID: GSE40395).

Statistical Analysis. GraphPad Prism (v. 5.0; GraphPad Software, La Jolla, CA) was used to perform a Mann-Whitney *U* test to compare data between two groups, and differences were considered statistically significant at $P < 0.05$.

All other materials and methods are described in the Supporting Information.

Results

Characteristics of the NASH Mouse Model. The pathological and clinical features of cirrhosis in patients are not well replicated by the majority of chemically induced murine cirrhotic liver models. We have established steatohepatitis as a cirrhotic liver mouse model by feeding mice an Ath+HF diet.[13] When mice were fed this diet for 34 weeks, hepatocytes developed steatosis, Mallory-Denk bodies, and ballooning (Fig. 1A,B), which are identical to typical pathological features of clinical NASH.[15] Albumin expression in parenchymal cells of the cirrhotic liver significantly decreased in mice fed the Ath+HF diet for 24 weeks (Fig. 1C), while alpha-fetoprotein (AFP) expression was not affected (Fig. 1D). Fibrosis developed and reached maximal levels after 34 weeks of feeding the Ath+HF diet (Fig. 1E,F). Immunohistochemical staining for immunomodulatory cells showed an increased number of Gr-1$^+$ cells in the liver of the steatohepatitis mice fed the Ath+HF diet for 12, 34, and 70 weeks (Fig. 2A,B). The number of CD11b$^+$ cells in the liver also increased and reached maximal levels after 34 weeks of feeding the Ath+HF diet (Fig. 2C,D). Thus, the murine cirrhosis model established by an Ath+HF diet mimics the features of clinical NASH.

Effect of ADSCs Treatment on Liver Albumin Expression and Fibrosis. Adipose tissue contains MSCs, which have the potential to differentiate into several types of cell lineages[10,14] and to act as immunomodulators.[11] In this study, we isolated stromal cells from inguinal adipose tissue of GFP-expressing transgenic (GFP-Tg) mice as ADSCs and expanded them in culture. The majority of these cells expressed CD90 and CD44, known surface markers of mesenchymal cells (Supporting Fig. 1A). A proportion of the expanded ADSCs also expressed CD105 (Supporting Fig. 1B), which has been recognized as a representative surface marker of MSCs.[11]

We evaluated whether ADSCs could provide a therapeutically beneficial treatment for liver cirrhosis in steatohepatitis mice. We injected 1 × 10^5 GFP-ADSCs by way of the spleen/portal vein in mice fed the Ath+HF diet for 32 weeks. We observed that the GFP-ADSCs resided in all lobes of the liver at 3, 7, and 14 days after injection (Fig. 3A,B). Importantly, immunohistochemical staining showed that GFP$^+$ cells in the cirrhotic liver expressed higher levels of albumin than did the surrounding parenchymal cells (Fig. 3C).

We also injected 1 × 10^5 or 2 × 10^4 GFP-ADSCs twice every 2 weeks by way of the splenic/portal vein

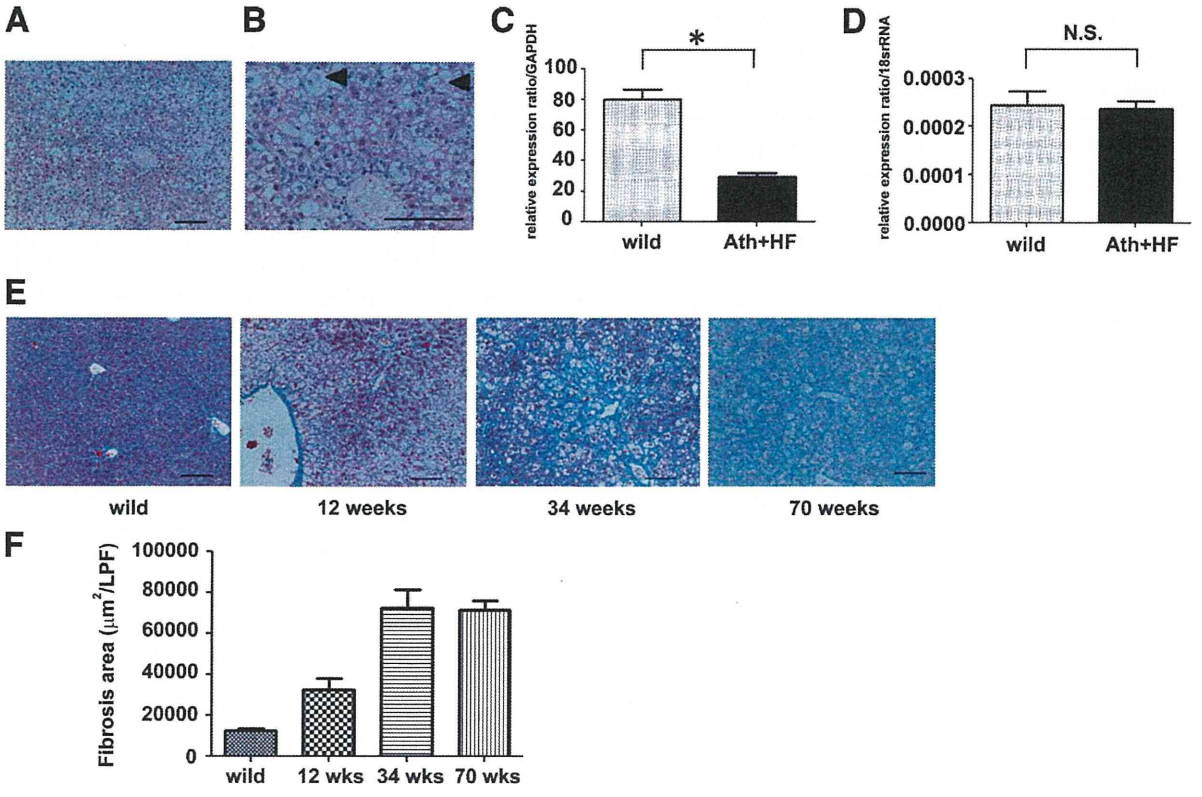

Fig. 1. Characteristics of the steatohepatitis murine model. Eight-week-old C57Bl/6 female mice were fed an Ath+HF diet. Liver tissue was obtained after 34 weeks, sectioned, and histologically examined with hematoxylin and eosin staining in (A,B) mice fed an Ath+HF diet for 34 weeks. Arrowheads indicate a Mallory-Denk body in a hepatocyte with ballooning. Parenchymal cells were isolated from 32-week-old C57Bl/6 wild-type female mice or Ath+HF mice that started the diet at 8 weeks old and continued for 24 weeks. Expression of (C) albumin and (D) AFP was assessed by reverse-transcription polymerase chain reaction (RT-PCR), n = 4, $*P < 0.05$. (E) Fibrosis was histologically examined with Azan staining in liver tissue of mice fed the Ath+HF diet for 12, 34, and 70 weeks. (F) Fibrosis areas of mice at 12, 34, and 70 weeks per ×100 low-power field were calculated for five visual fields. Bars: standard error. Scale bars = 100 μm.

in mice fed an Ath+HF diet for 32 or 36 weeks, respectively. Two weeks after the last injection the mice were euthanized and the therapeutic effects were assessed. The expression of albumin (Fig. 4A) was restored in hepatic parenchymal cells of cirrhotic mice at 2 weeks after the last injection, suggesting that ADSC treatment restored parenchymal cell function. The expression of AFP was also increased by ADSC treatment (Fig. 4B), implying enhanced regeneration of hepatic parenchymal cells. Similar effects were observed with a reduced number of (2×10^4) GFP-ADSCs (Supporting Fig. 2A,B).

We also assessed the effect of ADSC injection on fibrosis in cirrhotic mice. Liver tissue stained with Azan and anticollagen type IV antibody showed that ADSC administration reduced fibrosis compared to control animals (Fig. 5A,B; Supporting Fig. S3A,B). We also evaluated immunohistochemical staining of α-SMA, a marker of stellate cells, which are largely responsible for developing fibrosis. These results demonstrated that the number of α-SMA$^+$ cells was reduced by ADSC treatment (Fig. 5C-E), suggesting that ADSCs suppress the activity of stellate cells and ameliorate liver fibrosis.

Gene Expression Profiling of Cirrhotic Livers Following ADSC Treatment. We examined the gene expression profile of the livers in the NASH mouse model of cirrhosis by DNA microarray to determine whether administration of ADSCs was therapeutically beneficial. We identified expression of 1,249 gene probes that were significantly affected by ADSC injection. Clustering analysis of gene expression using these gene probes distinguished between ADSCs-treated mice and PBS-treated mice (Fig. 6A). Among 1,249 genes, 797 were up-regulated and 452 were down-regulated by ADSC treatment. Regarding matrix metalloproteinase (MMP), expressions of MMP-8 and MMP-9 were enhanced in the liver of NASH mice treated with PBS compared to the wild type; this enhancement was removed by ADSC treatment

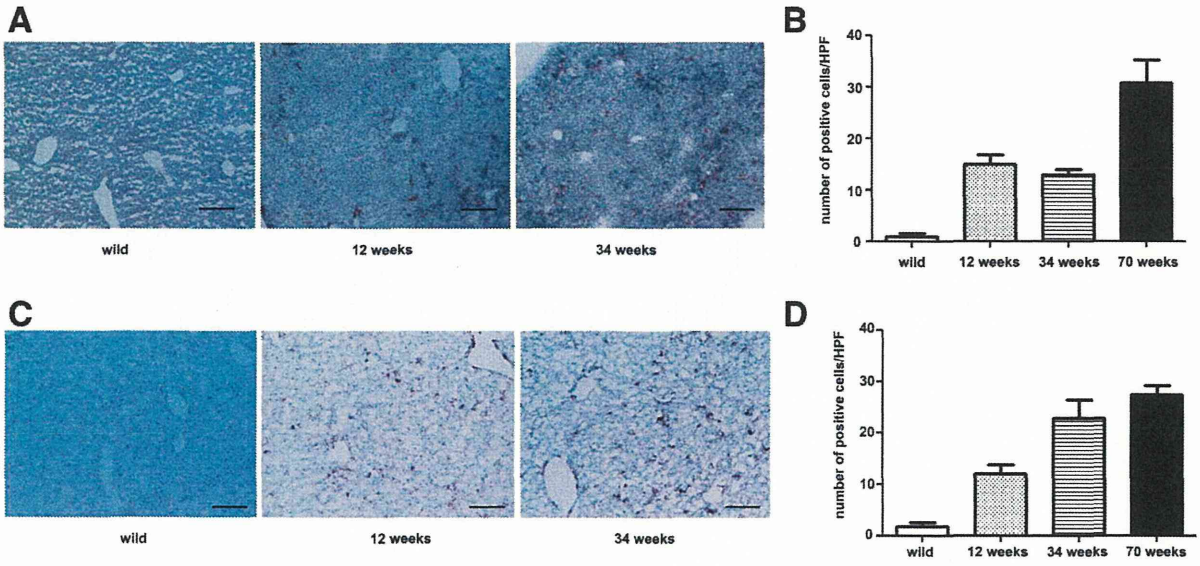

Fig. 2. Immunohistochemical staining of a steatohepatitis liver. Eight-week-old female C57Bl/6 female mice were fed an Ath+HF diet. Liver tissue was obtained from these mice or from wild-type animals after 12, 34, and 70 weeks. Immunohistochemical staining was performed for (A) Gr-1$^+$ or (C) CD11b$^+$ cells and the number of positive cells in a high-power field was counted for five visual fields for (B) Gr-1 or (D) CD11b at each timepoint.

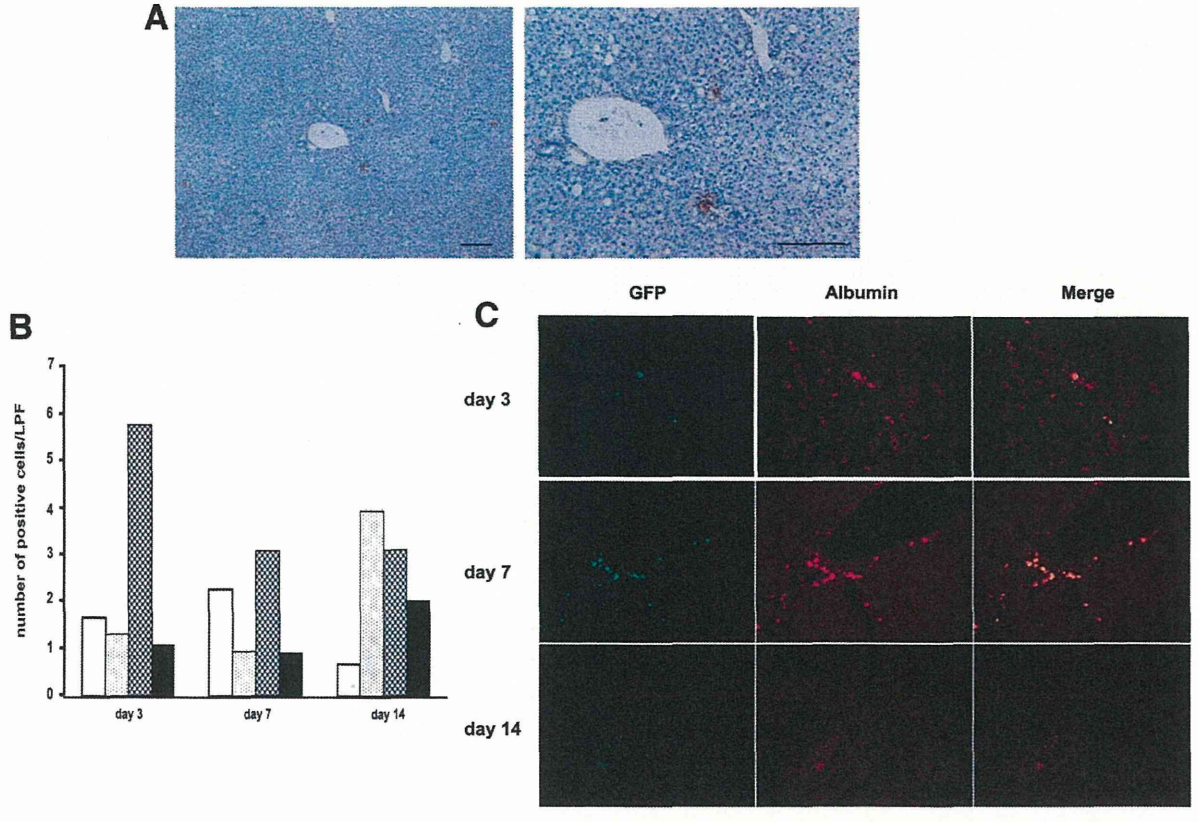

Fig. 3. Distribution of ADSCs and albumin expression in the livers of steatohepatitis mice. ADSCs from GFP-Tg mice (1×10^5) were injected into the splenic subcapsule of cirrhotic C57Bl/6 mice fed the Ath+HF diet for 32 weeks. After 3, 7, and 14 days, liver tissue was obtained and examined by immunohistochemical staining for (A) GFP; Scale bars = 100 μm. (B) GFP$^+$ cells in the liver were counted per ×100 low-power field and five visual fields were calculated. White bar, caudate lobe; dotted bar, left lobe; hatched bar, middle lobe; black bar, right lobe. (C) Immunohistochemical staining for GFP or albumin antibody. Magnification, ×100.

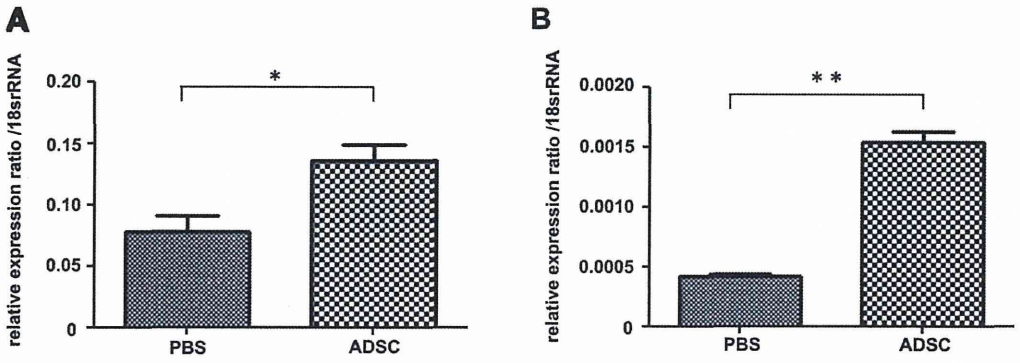

Fig. 4. Albumin and AFP expression in hepatic parenchymal cells. ADSCs from GFP-Tg mice (1×10^5) were injected twice every 2 weeks into the splenic subcapsule of cirrhotic C57Bl/6 mice fed an Ath+HF diet for 32 weeks. Control mice received PBS injections. Two weeks after the last injection, liver tissue was obtained and parenchymal cells were isolated for real-time PCR. Expressions of (A) albumin and (B) AFP were normalized relative to that of 18S ribosomal RNA (rRNA); $*P < 0.05$, $**P < 0.01$.

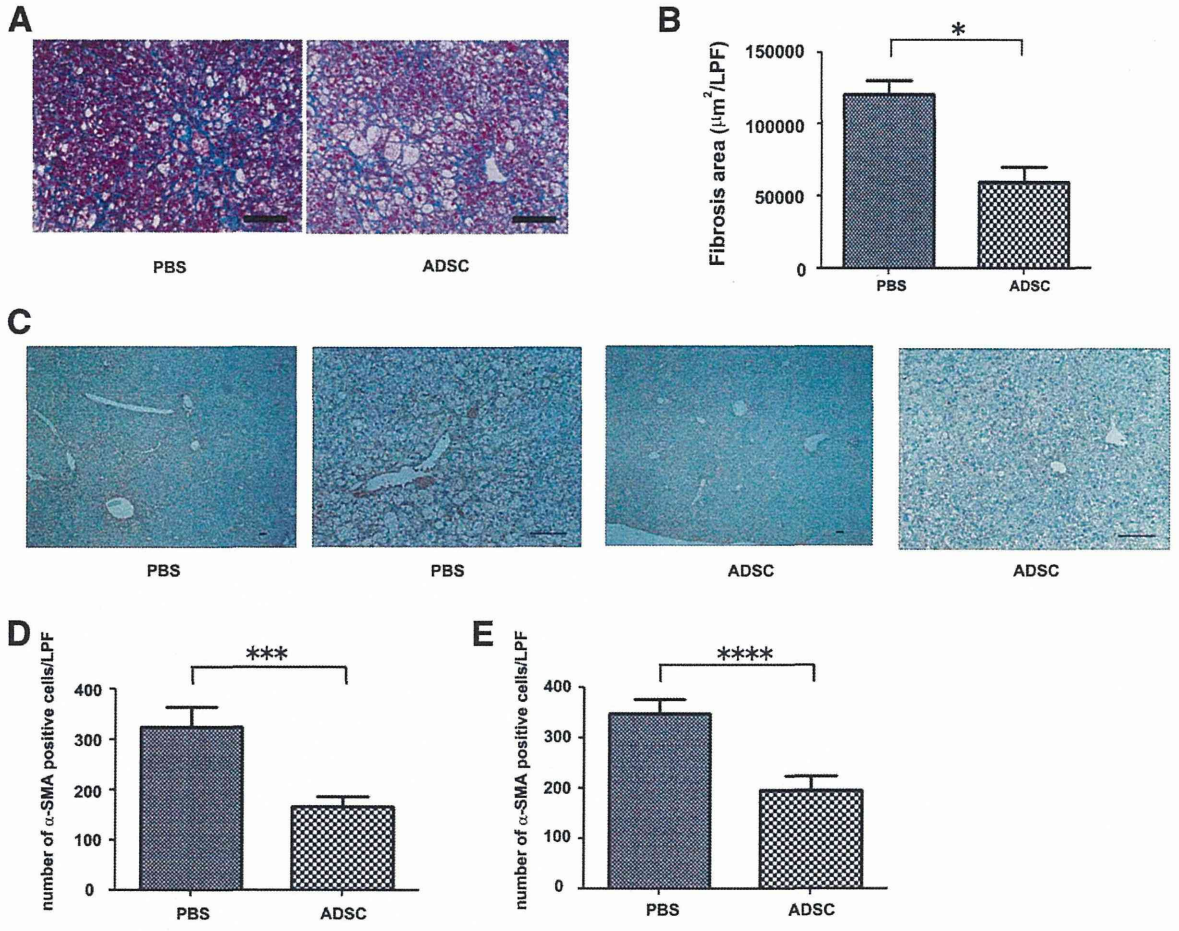

Fig. 5. Effect of ADSCs on liver fibrosis. ADSCs from GFP-Tg mice (1×10^5) were injected twice every 2 weeks into the splenic subcapsule of cirrhotic C57Bl/6 mice fed the Ath+HF diet for 32 weeks. Control mice received PBS injections. (A) Two weeks after the last injection, liver tissue was obtained, sectioned, and histologically examined with hematoxylin and eosin staining. (B) Fibrosis was examined by Azan staining and fibrotic area was quantified by image-analysis. (C) Immunohistochemical staining of liver sections for α-SMA. Scale bars = 100 μm. (D,E) The number of α-SMA+ cells in liver tissues obtained 1 (D) or 2 weeks (E) after the last ADSC injection determined by microscopy of five low-power fields (×100); $***P < 0.005$, $****P = 0.0001$.

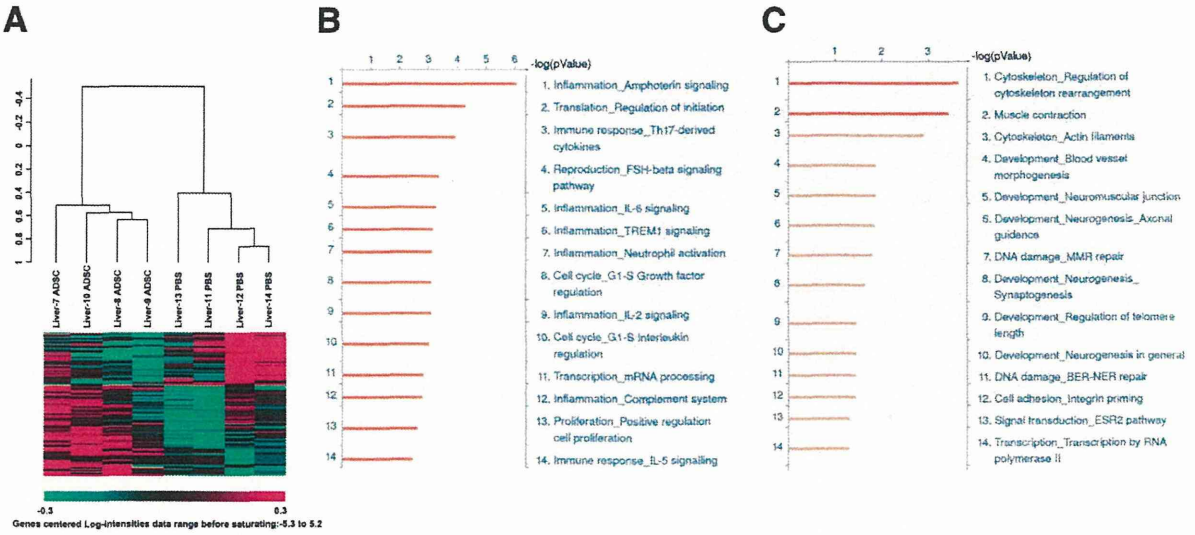

Fig. 6. Hepatic gene expression analysis. ADSCs from GFP-Tg mice (1×10^5) were injected twice every 2 weeks into the splenic subcapsule of cirrhotic C57Bl/6 mice fed an Ath+HF diet for 40 weeks. Control mice received PBS injections. Two weeks later, liver tissue was subjected to RNA isolation and gene expression using DNA microarrays. (A) Unsupervised clustering analysis was performed using probes for 1,249 genes whose expression differed significantly between the PBS and ADSC groups. (B) The biological processes of 452 genes whose expression was down-regulated in the ADSCs group compared to the PBS group were analyzed. (C) The biological processes of 797 genes whose expression was up-regulated in the ADSCs group compared to the PBS group were analyzed.

(Supporting Fig. S4). Biological process analysis indicated that the down-regulated genes were primarily related to inflammation and the immune response (Fig. 6B), and the up-regulated genes were related to tissue construction and development (Fig. 6C). Thus, gene expression analysis of liver tissue demonstrated that ADSCs treatment caused anti-inflammatory effects, as well as regeneration/repair effects, in the livers of a NASH mouse model of cirrhosis.

Anti-inflammatory Effects of ADSC Treatment. The fundamental underlying pathophysiology of steatohepatitis-induced cirrhosis is persistent hepatic inflammation caused by steatosis in hepatocytes.[16] We examined how ADSCs affected persistent inflammation of the liver in NASH mice at 2 weeks after the last injection of ADSCs. Immunohistochemical staining showed that the number of $CD11b^+$ cells accumulating in the livers of cirrhotic mice decreased with ADSC treatment compared to those of PBS-treated mice (Fig. 7A). The number of $Gr\text{-}1^+$ cells in cirrhotic liver also decreased with ADSC treatment (Fig. 7A), suggesting that ADSCs affect granulocytes and antigen-presenting cell lineage.

We further examined whether ADSC treatment affected the lymphocyte lineage of T cells, since they also play an important role in immune regulation of steatohepatitis.[17] We isolated lymphocytes from the livers of mice treated with ADSCs and examined the $CD4^+$ and $CD8^+$ T cells using flow cytometry. $CD8^+$ T cells were found predominantly in cirrhotic mice treated with PBS (Fig. 7B,C). However, when the mice were treated with ADSCs the number of $CD4^+$ T cells increased and was comparable to that of $CD8^+$ T cells, indicating that ADSC treatment affected T-cell subpopulations.

Gene Expression Profiling of Hepatic Inflammatory Cells Following ADSC Treatment. We further examined how injected ADSCs affected hepatic inflammatory cell gene expression by using DNA microarrays. By filtering the results from 5,065 gene probes, completely discernible clusters of gene expression were formed between ADSC- and PBS-treated animals (Fig. 8A). We identified the expression of 873 genes that were significantly up-regulated at least 2-fold with ADSC injection and 658 genes that were down-regulated. Most of the chemokines and cytokines whose expression was significantly affected by ADSCs were down-regulated (Supporting Table S1). Using the publicly available gene expression database for hematopoietic cells (GSE27787) and various types of helper T cells (GSE14308), we examined features of these affected genes in the context of immunomodulatory cells. Among the hematopoietic cells, genes with available symbol annotation were predominately $Gr\text{-}1^+$ and $CD11b^+$ cells from granulocyte and macrophage lineages (Fig. 8B). Among helper T-cell populations,

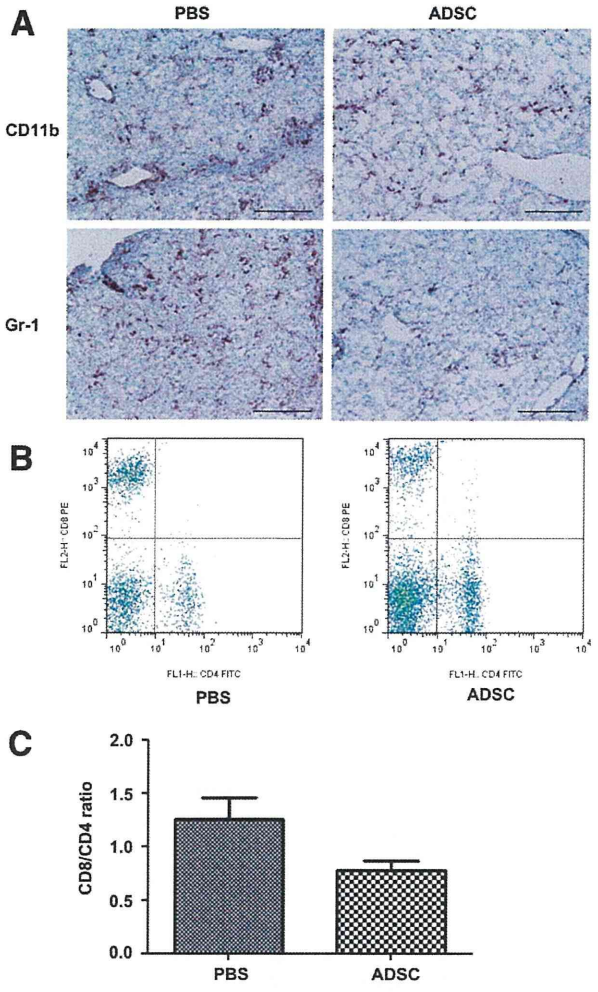

Fig. 7. Effect of ADSCs on inflammatory cells in the cirrhotic liver. ADSCs from GFP-Tg mice (1×10^5) were injected twice every 2 weeks into the splenic subcapsule of cirrhotic C57Bl/6 mice fed the Ath+HF diet for 32 weeks. Control mice received PBS injections. Two weeks later, liver tissue was obtained and immunohistochemical staining of (A) $CD11b^+$ and (B) $Gr\text{-}1^+$ cells was performed. Inflammatory cells in the liver were also isolated and stained with FITC-labeled anti-CD4 and PE-labeled CD8 antibodies. (C) The ratio of $CD8^+$ cells to $CD4^+$ cells was calculated. N = 4 ± standard error.

annotated genes included activated Th1, Th2, and Th17 cell types (Fig. 8C). We also isolated $CD4^+$T cells from hepatic inflammatory cells obtained from NASH mice fed an Ath+HF diet for 12 weeks, then treated with ADSC. Expressions of the Th1, Th2, and Th17 cytokines, interferon-γ, interleukin (IL)−4, IL-10, and IL-17, the Th17-related cytokine transforming growth factor beta (TGF-β), and Foxp3, a representative transcription factor of regulatory T cells, were down-regulated by ADSC treatment (Supporting Fig. S5).

These results suggest that ADSC treatment suppresses inflammation in the NASH mouse model primarily by down-regulating granulocytes, antigen-presenting cells, and activated helper T cells.

Discussion

This study investigated the therapeutic effect of ADSCs in a NASH murine model of cirrhosis. This model is relevant to clinical NASH, with similar pathological features established by an atherogenic high-fat diet, including the appearance of steatosis, ballooning, and Mallory-Denk bodies in hepatocytes, infiltration of inflammatory cells, and pericellular fibrosis. Our results demonstrate that ADSC injection is therapeutically beneficial for cirrhosis in this murine model through restoration of albumin expression in hepatic parenchymal cells, amelioration of fibrosis, and suppression of persistent hepatic inflammation.

Gene expression analysis of the liver in this cirrhotic mouse model revealed that ADSC injection affects biological processes relating to anti-inflammatory and regeneration/repair pathways. The anti-inflammatory effects are mediated by ADSC targeting of $Gr\text{-}1^+$, $CD11b^+$, and helper T-cell lineages. In patients with clinical NASH, the ratio of neutrophils to lymphocytes increases,[18] suggesting that granulocytes are involved in the pathogenesis of NASH. The NASH murine model used in this study produced an increased $CD8^+/CD4^+$ T-cell ratio, which is also comparable to clinical NASH patient pathology.[19] Gene expression analysis of liver tissue and hepatic inflammatory cells from NASH mice showed that Th1-, Th2-, and Th17-related genes were down-regulated by ADSC treatment. Helper T-cell activation skewed to produce Th1 cytokines is pathogenic in steatohepatitis.[20,21] In particular, Th17 is emerging as an important source of IL-17 family cytokines[22] and is involved in the hepatic inflammation in NASH.[23] Helper T cells producing Th2 cytokines such as IL-4, 5, and 13 contribute to fibrosis.[24] We conclude that activated T helper cells are responsible for the pathogenesis of steatohepatitis in the NASH murine model used in this study and that ADSCs suppress pathogenic helper T-cell activation. However, the suppression of miscellaneous effector and regulatory helper T cells by ADSCs should be further evaluated with regard to prevention of hepatocellular carcinoma, a frequent sequela to cirrhosis, since Th1 promotes antitumor immunity and Th2 down-regulates antitumor immunity.

We also observed that ADSC treatment ameliorated fibrosis and decreased the number of α-SMA^+ stellate

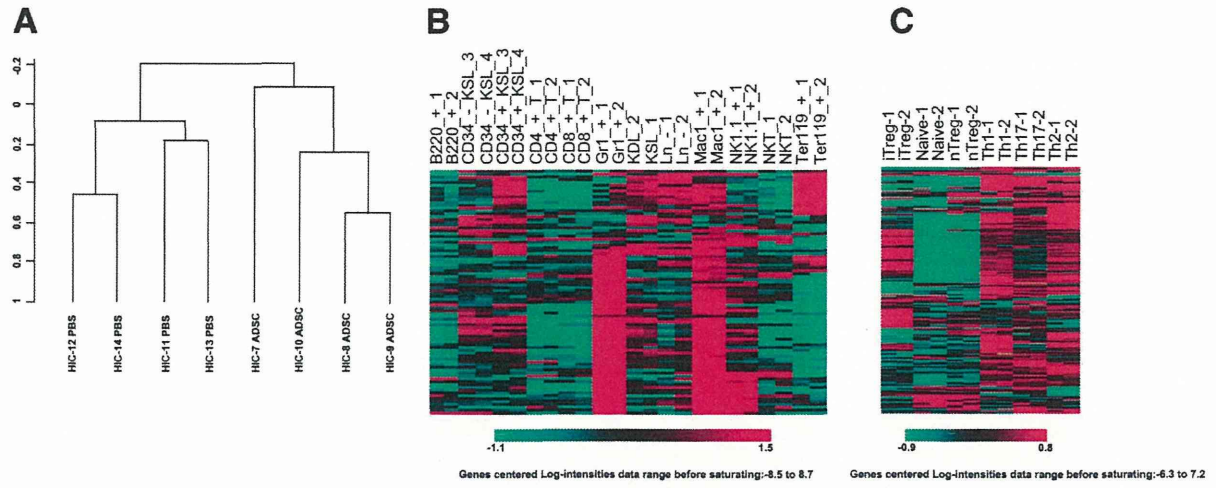

Fig. 8. Gene-expression analysis of intrahepatic inflammatory cells. ADSCs from GFP-Tg mice (1×10^5) were injected twice every 2 weeks into the splenic subcapsule of cirrhotic C57Bl/6 mice fed an Ath+HF diet for 40 weeks. Control mice received PBS injections. Inflammatory cells were isolated from the liver and gene expression examination was performed using DNA microarrays. (A) Unsupervised clustering analysis using the filtered 5,065 gene probes. HIC; hepatic inflammatory cells. (B) One-way clustering analysis using a publicly available database of hematopoietic cells (GSE27787) of 658 genes whose expression was down-regulated by ADSC treatment with available gene symbol annotations. (C) One-way clustering analysis using publicly available database of different helper T subsets (GSE14308) of 658 genes whose expression was down-regulated by ADSCs treatment with available gene symbol annotations.

cells in cirrhotic liver. When inflammation persists in the liver, fibrosis progresses due to these activated stellate cells, which are almost identical to myofibroblasts and produce extracellular matrix. Stellate cells are activated by miscellaneous factors including TGF-β and platelet-derived growth factor,[25] produced mostly from Kupffer cells. Helper T cells expressing Th2 cytokines are also involved in the development of fibrosis. Gene expression analysis of the cirrhotic livers indicated that ADSC treatment suppressed Th2-type helper T cells. Although details of how these molecules mediate fibrosis development have yet to be examined in the current NASH murine model, the antifibrotic effect of ADSCs is achieved in part by suppressing Th2-type helper T cells. We found that MMP-8 and MMP-9 enhancement in the NASH-cirrhotic liver was ameliorated by ADSC treatment. MMP-9 expression is related to the inflammation typical of steatohepatitis[26] and can ameliorate the hepatic fibrosis induced by carbon tetrachloride.[27] Further studies are needed to clarify the role of MMPs in the pathogenesis of cirrhosis as well as to explore novel therapies for this condition.

Pluripotent MSCs differentiate into several cell lineages and are a promising avenue for regenerative therapy of various impaired organs, including the liver. Although ADSCs were observed in cirrhotic livers at up to 2 weeks after injection and expressed albumin, the numbers of resident cells were not sufficient to supplement hepatic function. Therefore, pluripotency, as well as the anti-inflammatory and antifibrotic effects of ADSCs, are important for their regenerative/repair effects in liver cirrhosis. Rather than studying the effects of ADSCs on early-stage steatohepatitis, we treated mice with endstage cirrhosis with ADSCs to observe their therapeutic effects. Our results demonstrated that ADSCs can effectively resolve chronic fibrosis and decrease inflammation, thereby restoring hepatic function in endstage cirrhotic mice, implying the usefulness of this therapy as an alternative to liver transplantation.

In conclusion, ADSCs proved therapeutically beneficial and clinically relevant in regenerative therapy of a murine steatohepatitis-cirrhosis model. Clinical application of ADSCs in the treatment of cirrhosis is expected to provide a novel alternative regenerative/repair therapy for patients with cirrhosis.

References

1. D'Amico G, Garcia-Tsao G, Pagliaro L. Natural history and prognostic indicators of survival in cirrhosis: a systematic review of 118 studies. J Hepatol 2006;44:217-231.
2. Llovet JM, Burroughs A, Bruix J. Hepatocellular carcinoma. Lancet 2003;362:1907-1917.
3. Fattovich G, Stroffolini T, Zagni I, Donato F. Hepatocellular carcinoma in cirrhosis: incidence and risk factors. Gastroenterology 2004;127:S35-50.
4. Kamath PS, Kim WR. The model for end-stage liver disease (MELD). Hepatology 2007;45:797-805.
5. Stravitz RT, Carl DE, Biskobing DM. Medical management of the liver transplant recipient. Clin Liver Dis 2011;15:821-843.

6. Forner A, Llovet JM, Bruix J. Hepatocellular carcinoma. Lancet 2012;379:1245-1255.
7. Chamberlain G, Fox J, Ashton B, Middleton J. Concise review: mesenchymal stem cells: their phenotype, differentiation capacity, immunological features, and potential for homing. Stem Cells 2007;25:2739-2749.
8. Franco Lambert AP, Fraga Zandonai A, Bonatto D, Cantarelli Machado D, Pegas Henriques JA. Differentiation of human adipose-derived adult stem cells into neuronal tissue: does it work? Differentiation 2009;77:221-228.
9. Banas A, Teratani T, Yamamoto Y, Tokuhara M, Takeshita F, Osaki M, et al. Rapid hepatic fate specification of adipose-derived stem cells and their therapeutic potential for liver failure. J Gastroenterol Hepatol 2009;24:70-77.
10. Banas A, Teratani T, Yamamoto Y, Tokuhara M, Takeshita F, Quinn G, et al. Adipose tissue-derived mesenchymal stem cells as a source of human hepatocytes. HEPATOLOGY 2007;46:219-228.
11. Uccelli A, Moretta L, Pistoia V. Immunoregulatory function of mesenchymal stem cells. Eur J Immunol 2006;36:2566-2573.
12. Zuk PA, Zhu M, Ashjian P, De Ugarte DA, Huang JI, Mizuno H, et al. Human adipose tissue is a source of multipotent stem cells. Mol Biol Cell 2002;13:4279-4295.
13. Matsuzawa N, Takamura T, Kurita S, Misu H, Ota T, Ando H, et al. Lipid-induced oxidative stress causes steatohepatitis in mice fed an atherogenic diet. HEPATOLOGY 2007;46:1392-1403.
14. Furuichi K, Shintani H, Sakai Y, Ochiya T, Matsushima K, Kaneko S, et al. Effects of adipose-derived mesenchymal cells on ischemia-reperfusion injury in kidney. Clin Exp Nephrol 2012;16:579-589.
15. Brunt EM. Nonalcoholic steatohepatitis: definition and pathology. Semin Liver Dis 2001;21:3-16.
16. Cohen JC, Horton JD, Hobbs HH. Human fatty liver disease: old questions and new insights. Science 2011;332:1519-1523.
17. Inzaugarat ME, Ferreyra Solari NE, Billordo LA, Abecasis R, Gadano AC, Chernavsky AC. Altered phenotype and functionality of circulating immune cells characterize adult patients with nonalcoholic steatohepatitis. J Clin Immunol 2011;31:1120-1130.
18. Alkhouri N, Morris-Stiff G, Campbell C, Lopez R, Tamimi TA, Yerian L, et al. Neutrophil to lymphocyte ratio: a new marker for predicting steatohepatitis and fibrosis in patients with nonalcoholic fatty liver disease. Liver Int 2012;32:297-302.
19. Susca M, Grassi A, Zauli D, Volta U, Lenzi M, Marchesini G, et al. Liver inflammatory cells, apoptosis, regeneration and stellate cell activation in non-alcoholic steatohepatitis. Dig Liver Dis 2001;33:768-777.
20. Olleros ML, Martin ML, Vesin D, Fotio AL, Santiago-Raber ML, Rubbia-Brandt L, et al. Fat diet and alcohol-induced steatohepatitis after LPS challenge in mice: role of bioactive TNF and Th1 type cytokines. Cytokine 2008;44:118-125.
21. Ferreyra Solari NE, Inzaugarat ME, Baz P, De Matteo E, Lezama C, Galoppo M, et al. The role of innate cells is coupled to a Th1-polarized immune response in pediatric nonalcoholic steatohepatitis. J Clin Immunol 2012;32:611-621.
22. Ouyang W, Kolls JK, Zheng Y. The biological functions of T helper 17 cell effector cytokines in inflammation. Immunity 2008;28:454-467.
23. Tang Y, Bian Z, Zhao L, Liu Y, Liang S, Wang Q, et al. Interleukin-17 exacerbates hepatic steatosis and inflammation in non-alcoholic fatty liver disease. Clin Exp Immunol 2011;166:281-290.
24. Wynn TA. Fibrotic disease and the T(H)1/T(H)2 paradigm. Nat Rev Immunol 2004;4:583-594.
25. Wu J, Zern MA. Hepatic stellate cells: a target for the treatment of liver fibrosis. J Gastroenterol 2000;35:665-672.
26. Wanninger J, Walter R, Bauer S, Eisinger K, Schaffler A, Dorn C, et al. MMP-9 activity is increased by adiponectin in primary human hepatocytes but even negatively correlates with serum adiponectin in a rodent model of non-alcoholic steatohepatitis. Exp Mol Pathol 2011;91:603-607.
27. Higashiyama R, Inagaki Y, Hong YY, Kushida M, Nakao S, Niioka M, et al. Bone marrow-derived cells express matrix metalloproteinases and contribute to regression of liver fibrosis in mice. HEPATOLOGY 2007;45:213-222.

JVI
Journals.ASM.org

MicroRNA-27a Regulates Lipid Metabolism and Inhibits Hepatitis C Virus Replication in Human Hepatoma Cells

Takayoshi Shirasaki,[a,b] Masao Honda,[a,b] Tetsuro Shimakami,[a] Rika Horii,[a] Taro Yamashita,[a] Yoshio Sakai,[a] Akito Sakai,[a] Hikari Okada,[a] Risa Watanabe,[b] Seishi Murakami,[a] MinKyung Yi,[c] Stanley M. Lemon,[d] Shuichi Kaneko[a]

Department of Gastroenterology, Kanazawa University Graduate School of Medical Science, Kanazawa, Japan[a]; Department of Advanced Medical Technology, Kanazawa University Graduate School of Health Medicine, Kanazawa, Japan[b]; Human Center for Hepatitis Research, Institute for Human Infections and Immunity, and Department of Microbiology and Immunology, University of Texas Medical Branch, Galveston, Texas, USA[c]; Division of Infectious Diseases, School of Medicine, The University of North Carolina at Chapel Hill, Chapel Hill, North Carolina, USA[d]

The replication and infectivity of the lipotropic hepatitis C virus (HCV) are regulated by cellular lipid status. Among differentially expressed microRNAs (miRNAs), we found that miR-27a was preferentially expressed in HCV-infected liver over hepatitis B virus (HBV)-infected liver. Gene expression profiling of Huh-7.5 cells showed that miR-27a regulates lipid metabolism by targeting the lipid synthetic transcription factor RXRα and the lipid transporter ATP-binding cassette subfamily A member 1. In addition, miR-27a repressed the expression of many lipid metabolism-related genes, including *FASN*, *SREBP1*, *SREBP2*, *PPARα*, and *PPARγ*, as well as *ApoA1*, *ApoB100*, and *ApoE3*, which are essential for the production of infectious viral particles. miR-27a repression increased the cellular lipid content, decreased the buoyant density of HCV particles from 1.13 to 1.08 g/cm^3, and increased viral replication and infectivity. miR-27a overexpression substantially decreased viral infectivity. Furthermore, miR-27a enhanced *in vitro* interferon (IFN) signaling, and patients who expressed high levels of miR-27a in the liver showed a more favorable response to pegylated IFN and ribavirin combination therapy. Interestingly, the expression of miR-27a was upregulated by HCV infection and lipid overload through the adipocyte differentiation transcription factor C/EBPα. In turn, upregulated miR-27a repressed HCV infection and lipid storage in cells. Thus, this negative feedback mechanism might contribute to the maintenance of a low viral load and would be beneficial to the virus by allowing it to escape host immune surveillance and establish a persistent chronic HCV infection.

MicroRNA (miRNA) is a small, endogenous, single-stranded, noncoding RNA consisting of 20 to 25 bases that regulates gene expression. It plays an important role in various biological processes, including organ development, differentiation, and cellular death and proliferation, and is also involved in infection and diseases such as cancer (1).

Previously, we examined miRNA expression in hepatocellular carcinoma (HCC) and noncancerous background liver tissue infected with hepatitis B virus (HBV) and HCV (2). We showed that some miRNAs were differentially expressed according to HBV or HCV infection but not according to the presence of HCC. These infection-specific miRNAs were believed to regulate HBV or HCV replication; however, their functional role has not been elucidated.

HCV is described as a lipotropic virus because of its association with serum lipoprotein (3–5). It utilizes the low-density lipoprotein (LDL) receptor for cellular entry (6–8) and forms replication complexes on lipid rafts (9). The HCV core protein surrounds and binds lipid droplets (LDs) and nonstructural proteins on the endoplasmic reticulum (ER) membrane, which is essential for particle formation (10). Moreover, HCV cellular secretion is linked to very LDL (VLDL) secretion (11). In liver tissue histology, steatosis is often observed in chronic hepatitis C (CH-C) and is closely related to resistance to interferon (IFN) treatment (12, 13). Thus, lipids play important roles in HCV replication and CH-C pathogenesis.

Several miRNAs, such as miR-122 (14), miR-199a (15), miR-196 (16), miR-29 (17), Let-7b (18), and miR-130a (19), reportedly regulate HCV replication; however, miRNAs that regulate lipid metabolism and HCV replication have not been reported so far. Previously, we reported that 19 miRNAs were differentially expressed in HBV- and HCV-infected livers (2). In the present study, we evaluated the functional relevance of miR-27a in HCV replication by using the human hepatoma cell line Huh-7.5. We analyzed the regulation of lipid metabolism by miR-27a in hepatocytes and revealed a unique pathophysiological relationship between lipid metabolism and HCV replication in CH-C.

MATERIALS AND METHODS

Cell line. Huh-7.5 cells (kindly provided by C. M. Rice, Rockefeller University, New York, NY) were maintained in Dulbecco's modified Eagle's medium (DMEM; Gibco BRL, Gaithersburg, MD) containing 10% fetal bovine serum (FBS) and 1% penicillin-streptomycin.

HCV replication analysis. HCV replication analysis was performed by transfecting Huh-7.5 cells with JFH-1 (20), H77Sv2 Gluc2A (21), and their derivative RNA constructs. pH77Sv2 is a modification of pH77S, a plasmid containing the full-length sequence of the genotype 1a H77 HCV strain with five cell culture-adaptive mutations that promote its replication in Huh-7 hepatoma cells (21–24). pH77Sv2 Gluc2A is a related construct in which the *Gaussia* luciferase (Gluc) sequence, fused to the 2A autocatalytic protease of foot-and-mouth virus RNA, was inserted in frame between p7 and NS2 (21, 23, 25). pH77Sv2 Gluc2A (AAG) is a control plasmid that has an NS5B polymerase catalytic domain mutation.

Received 29 October 2012 Accepted 21 February 2013
Published ahead of print 28 February 2013
Address correspondence to Masao Honda, mhonda@m-kanazawa.jp.

doi:10.1128/JVI.03022-12